JOURNAL OF MATERIALS SCIENCE 18 (1983) 3633–3648

Synthesis of continuous silicon carbide fibre

Part 3 *Pyrolysis process of polycarbosilane and structure of the products*

YOSHIO HASEGAWA
The Research Institute for Special Inorganic Materials, Asahi-mura, Kashima-gun, Ibaraki-ken, 311-14, Japan

KIYOHITO OKAMURA
The Oarai Branch, The Research Institute for Iron, Steel and Other Metals, Tohoku University, Oarai, Ibaraki-Ken, 311-13, Japan

Polycarbosilanes which are the precursors of SiC fibre were synthesized by three methods. The molecular structure of each polycarbosilane was represented by means of three structural elements determined by IR, UV and NMR spectral measurements. The pyrolysis process of the polycarbosilanes is discussed for the six stages observed in the TG–DTA curves and gas evolution curves during pyrolysis of the polycarbosilanes. In each stage, the relationship between the molecular structure and the structure of the pyrolysis product is discussed and the pyrolysis process of the polycarbosilanes is characterized.

1. Introduction

We have reported previously the molecular structures of two polycarbosilanes (PC) and mechanical properties of the SiC fibres synthesized from these precursors [1, 2]. Another polycarbosilane was also synthesized by a method different from the two methods, and the mechanical properties of the SiC fibre obtained were reported [3]. These SiC fibres have high strength and high heat resistivity; their application as reinforcements in fibre-reinforced composite materials is expected [4]. However, when the cured PC fibres are heat treated above 1200° C, the strength of the SiC fibres decreases [5]. β-SiC crystallization in the fibres at high temperature is suggested as a factor for the decrease in strength. In order to elucidate such changes, the conversion process of PC into SiC and the relationship between the process and the fibre properties must be studied in detail. The relationship between the fibre structure and the mechanical properties has not yet been clarified. This is because it is difficult to determine the molecular structure of PC and to measure the structural changes in PC during the pyrolysis process.

In the present work, characterization of PCs synthesized by three different methods was made by comparative studies of the properties of these three PCs. On the basis of the results, the pyrolysis process of PCs and structure of the pyrolysis products are discussed.

2. Experimental details

2.1. Synthesis of polycarbosilanes

Three PCs were synthesized by three respective methods. PC was first synthesized by thermal decomposition and condensation of polydimethylsilane (PDMS) in an autoclave at 470° C for 14 h and condensation by removal of the components with low boiling points up to 280° C/1 mm Hg from the product by vacuum distillation (PC-470) [1]. PC was then synthesized by thermal decomposition and condensation of tetramethylsilane (TMS) for 24 h, recycling the vapour into a quartz tube heated at 770° C, as in the Fritz *et al.* method [6], and condensation by removal of the components with boiling points up to 200° C/1 mm Hg from product by vacuum distillation (PC–TMS) [2]. Another PC was synthesized by thermal decomposition and condensation of 2000 g PDMS

0022–2461/83 $03.00 + .12

added with 5.5 wt % borodiphenylsiloxane (BDPSO) in a stainless steel reaction vessel with a reflux condenser with outer temperature 450° C, holding the inner temperature at about 350° C, for 10.5 h under nitrogen gas flow. The product was dissolved in xylene and the solution was filtered to remove the insoluble. The components with boiling points up to 320° C were removed by distillation in nitrogen gas. 1300 g of PC (PC-B5.5) was thus obtained. PC-B3.2 was similarly obtained from PDMS added with 3.2 wt % BDPSO by thermal decomposition and condensation, and removal of the components with boiling points up to 280° C/1 mm Hg by vacuum distillation [3].

BDPSO was synthesized by reacting diphenyldichlorosilane (3 mol) with boric acid (1 mol) in *n*-butylether at 100° C for 18 h under nitrogen flow and then removing *n*-butylether by distillation after adding a little water and further heating up to 350° C.

For PC-470, PC–TMS and PC-B obtained by the above three methods, the following experiments were performed.

2.2. Characterization of polycarbosilanes

The structure of each PC was analysed by infrared (IR), ultraviolet (UV), and ^{1}H and ^{29}Si nuclear magnetic resonance (NMR) spectroscopy measurements of number-average molecular weight and molecular weight distribution, and chemical analysis.

IR spectra were measured by the KBr or KI pellet method with a Hitachi 295 infrared spectrophotometer.

UV spectra were measured in *n*-hexane solution with a Shimadzu MPS-5000 multipurpose recording spectrophotometer.

^{1}H and ^{29}Si NMR spectra were measured with a JEOL JNM-FX60 high-resolution FT NMR spectrometer at 60 MHz for ^{1}H and at 11.9 MHz for ^{29}Si, in $CDCl_3$ solution, using TMS as the internal standard.

Number-average molecular weights ($\bar{M}_n$) were measured with Hitachi 117 molecular weight apparatus by the vapour pressure osmometry method in benzene solution.

Molecular weight distributions were measured using Hitachi HLC-635A with Shodex A-80M as a GPC column in THF solution.

Chemical analyses were done for silicon, carbon, hydrogen, oxygen, and boron.

2.3. Characterization of pyrolysis of polycarbosilanes

TG–DTA curves of polycarbosilanes were obtained to examine the profile of the pyrolysis process with a high-temperature type Rigaku micro TG-DTA in 50 $cm^3 min^{-1}$ nitrogen flow up to 1300° C, at a heating rate of 5° C min^{-1}. Changes of pressure in the system were measured with a Pirani gauge to observe gas evolution when PC was heat treated up to 1500° C in a vacuum at a heating rate of 100° C h^{-1}.

The pyrolysis products were obtained every 100° C from 400 to 1500° C for 3.0 g PC in a high-purity alumina boat at a heating rate of 100° C h^{-1} in a vacuum under 3×10^{-3} torr. The keeping time at each heat-treatment temperature was 1 h. For these samples, measurements of the IR spectrum, X-ray diffraction pattern, number-average molecular weight and molecular weight distribution, and chemical analysis were made.

X-ray diffraction patterns were obtained with a Rigaku X-ray diffractometer using Cu$K\alpha$ radiation with a nickel-filter as the characteristic X-rays. Samples were pulverized in an agate mortar. Correction of the diffraction angle was made using silicon.

Other measurements were made by methods similar to those in Section 2.2.

For characterization of the pyrolysis process of PCs, the following treatment was applied to the IR spectra and X-ray diffraction patterns.

The pyrolysis process of organic compounds is represented by the change in the absorbance, A, of a characteristic absorption in the IR spectrum. The absorbance is given by the formula $A = \log(I_0/I)$ where I_0 and I are the intensities of the incident and the transmitted light. If Lambert–Berr's law holds, $A = Kcl$ where K is the extinction coefficient, c the concentration and l the thickness of an absorber. In the KBr pellet method, it is difficult to determine c and l exactly. Therefore, the pyrolysis process of PCs was shown in the heat-treatment temperature dependence of the ratio $A\bar{\nu}/A\bar{\nu}'$; $A\bar{\nu}$ and $A\bar{\nu}'$ are absorbances of the characteristic absorption at wave number $\bar{\nu}$ and $\bar{\nu}'$, respectively, in the spectrum of samples heat treated at each temperature. In the temperature range up to 600° C, the absorption at 2950 cm^{-1} (C–H stretch) was selected as the characteristic absorption at $\bar{\nu}'$ without overlapping with other absorptions, and the wave numbers 2100 cm^{-1} (Si–H stretch), 1355 cm^{-1} (CH_2 deformation of Si–CH_2–Si) and

1250 cm^{-1} (Si–Me deformation) [1, 2] were selected as $\bar{\nu}$.

In the X-ray diffraction pattern of the pyrolysis products of PC, the apparent crystalline size L_{111} was calculated from the half-width β of the (1 1 1) line of the β–SiC using Scherrer's formula $L_{111} = 1.0\lambda/(\beta \cos\theta)$ where λ is the wavelength of X-rays and θ the diffraction angle, and the relationship between L_{111} and heat-treatment temperature was examined.

3. Results and discussion

3.1. Characterization of polycarbosilanes

The structure of PCs can be discussed qualitatively by using IR and UV spectra.

The infrared spectrum of each PC is shown in Fig. 1. The absorption peaks at 2100 cm^{-1} (Si–H) and 1350 and 1020 cm^{-1} (Si–CH_2–Si) are common to PC–TMS, PC-470, PC-B3.2 and PC-B5.5. These peaks are characteristic showing that carbosilane is produced from TMS or PDMS [1, 2]. The comparison of intensities of the peaks at 1350 cm^{-1} and those at 1400 cm^{-1} (Si–CH_3) shows that the ratio of the number of Si–CH_3 bonds to that of Si–CH_2–Si bonds in PC–TMS and PC-470 is different from that in PC-B. And, in the comparison of intensities of the peaks at 2100 cm^{-1} and those at 2950 cm^{-1} (C–H), the relative intensity of the peak at 2100 cm^{-1} in PC-470 is particularly large compared with those in the other PCs. It is thus seen that the number of Si–H bonds in PC-B3.2 and in PC-B5.5 is smaller than in PC-470, in accordance with the previous result that the number of silicon atoms with a Si–H bond in the PC–TMS is smaller than in PC-470 [2]. From the IR spectra, it is found that the quantity of the substituent groups, that is H, CH_3 and $-CH_2-$, on the silicon atom, is different among the three PCs.

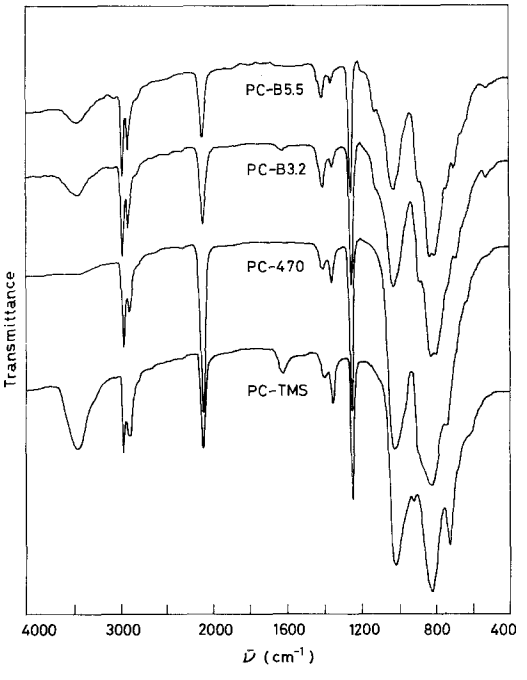

Figure 1 IR spectra of polycarbosilanes.

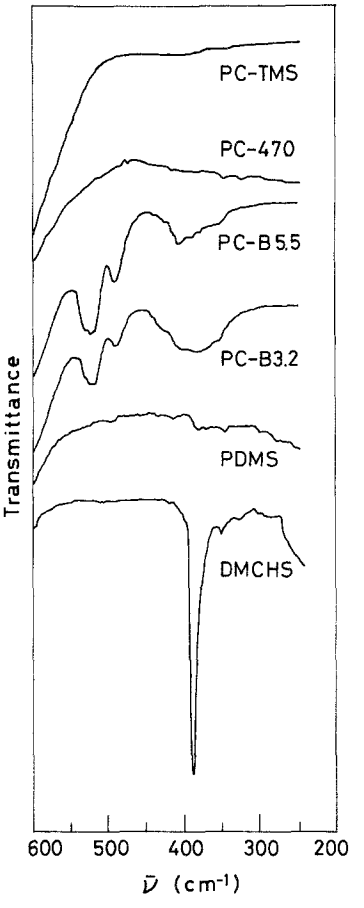

Figure 2 Far infrared spectra of polycarbosilanes, DMCHS and PDMS.

The far infrared spectra of PCs are shown in Fig. 2. The spectra of dodecamethylcyclohexasilane (DMCHS) and PDMS are also shown for comparison in Fig. 2. In the far infrared spectra, it is reported that cyclic or cage polysilane has an absorption peak in the range of 350 to 450 cm^{-1} due to the Si–Si stretching vibration [7, 8]; DMCHS has a sharp peak at 387 cm^{-1}. PDMS has no peak in this range because of the linear polysilane. Both PC–TMS and PC-470 have no peak in the range of 350 to 450 cm^{-1}, but PC-B3.2 and

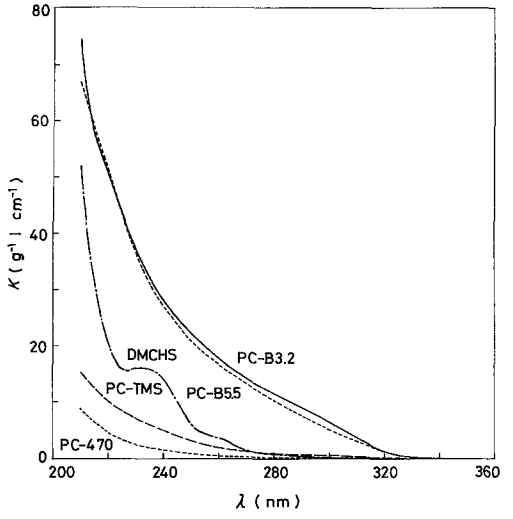

Figure 3 UV absorption spectra of polycarbosilanes and DMCHS.

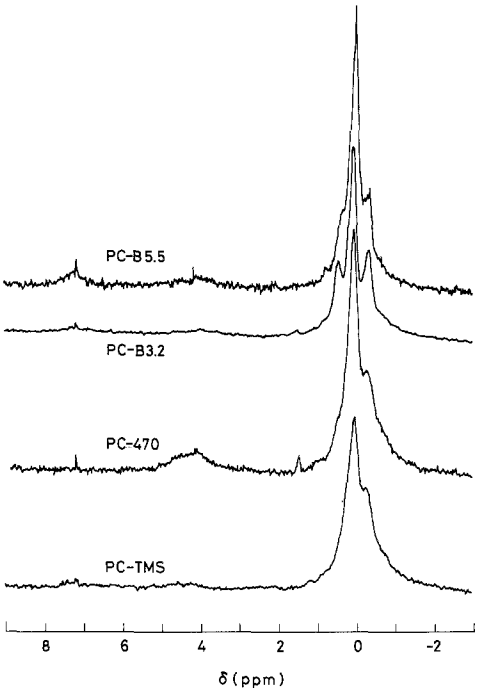

Figure 4 ^{1}H NMR spectra of polycarbosilanes.

PC-B5.5 have a broad peak in this range. It is shown that PC-B3.2 and PC-B5.5 have a cyclic or cage polysilane skeleton in the molecule.

Information about the Si–Si bond, including the linear polysilane skeleton, is obtained from UV spectra [7–9]. The UV spectra of PCs and DMCHS are shown in Fig. 3. PC-B exhibits far greater UV absorption than PC–TMS and PC-470, whose extinction coefficients are larger than those of all cyclic and cage polysilanes [7, 8]. It is indicated that PC-B3.2 and PC-B5.5 have a linear polysilane skeleton in the molecule [6]. This is possibly because low molecular weight polysilanes, produced by thermal decomposition and condensation of PDMS, is partly introduced in PC-B3.2 and PC-B5.5 molecules. In contrast, the intensity of UV absorption is small in PC–TMS and PC-470, so that the Si–Si bond does not exist or is very small.

As above, the retention of the polysilane skeleton in the molecule was shown by far infrared and UV spectra. These results will be discussed quantitatively.

Proton magnetic resonance (^{1}H NMR) spectra are shown in Fig. 4. In all PCs, a large peak centred at 0 ppm and a small peak in the 4 to 4.5 ppm range are observed; the former is due to (C)–H in Si–CH_3, Si–CH_2–, etc. and the latter to (Si)–H [6, 10, 11]. From the integral of the peaks, the ratio of the C–H to the Si–H bond can be calculated, as in Table I.

The ^{29}Si NMR spectra of PCs are shown in Fig. 5. The spectra of DMCHS, hexamethyldisilane (HMDS), hexamethyldisiloxane (HMDSO) and polydimethylsiloxane (PDMSO) are also shown for comparison. The spectra in Fig. 5b are the proton decoupling spectra. In the figure, the signals in the lower magnetic field than TMS (0 ppm) are shown by a positive sign. The proton decoupling spectra of PC–TMS, PC-470, PC-B3.2, PC-B5.5, DMCHS and HMDS show downward peaks due to a negative nuclear Overhowser effect (NOE), whereas in HMDSO, PDMSO and TMS the peaks are upward.

For comparison of Figs. 5a and b, the ^{29}Si NMR data of the PCs are given in Table II [6, 12]. The peak at −0.75 ppm observed in PC–TMS and in PC-470 is due to ^{29}Si without coupling with ^{1}H, since the position of the peak does not shift

TABLE I C–H/Si–H, SiC_4/SiC_3H and $SiC_xSi_{4-x}/(SiC_4 + SiC_3H)$ in polycarbosilane molecules

	PC–TMS	PC-470	PC-B3.2	PC-B5.5
C–H/Si–H	52.6	11.2	20.4	16.4
SiC_4/SiC_3H	6.33	1.04	–	–
$SiC_xSi_{4-x}/(SiC_4 + SiC_3H)$	0	0	0.159	0.130

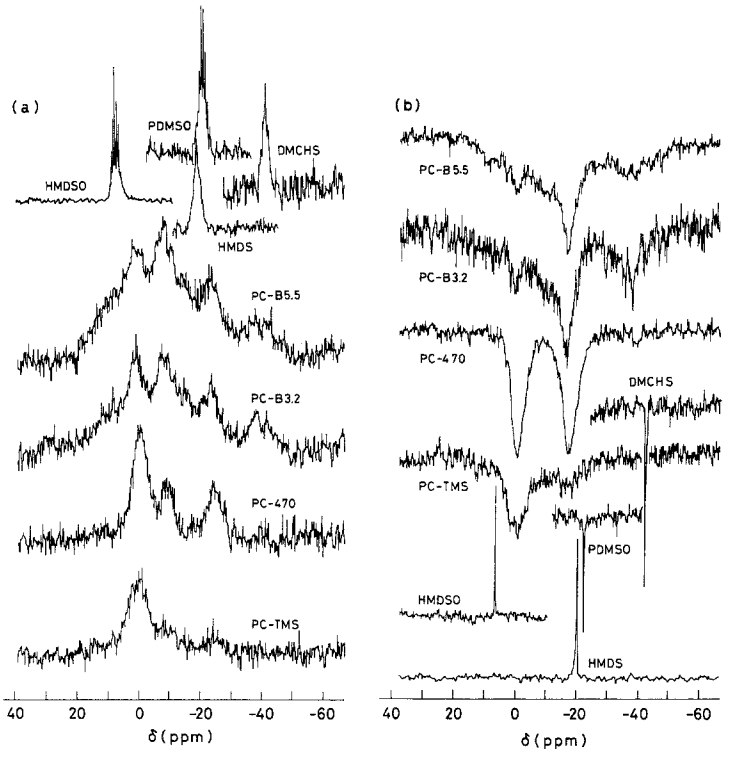

Figure 5 (a) ^{29}Si NMR spectra and (b) ^{1}H decoupling ^{29}Si NMR spectra of polycarbosilanes, HMDS, DMCHS, HMDSO and PDMSO.

regardless of the coupling or decoupling with a proton. As described later, this ^{29}Si atom does not bond with a silicon atom, so that the silicon atom should be bonded only with carbon atoms; it is hereafter called SiC_4. Similarly, the peak at 0.50 ppm in PC-B3.2 and PC-B5.5 is also due to a silicon atom of SiC_4. The peak at -17.50 ppm in PC–TMS and in PC-470 in Fig. 5b is separated into two peaks due to ^{29}Si coupling with one ^{1}H ($J_{^{29}Si-H} = 182$ Hz) [6], so that the silicon atom should be bonded with one hydrogen atom and three carbon atoms; it is called SiC_3H. Similarly, the peaks at -16.01 and -16.43 ppm in PC-B3.2 and in PC-B5.5 are due to a ^{29}Si atom of SiC_3H ($J_{^{29}Si-H} = 180$ Hz). The ratio of SiC_4 to SiC_3H is calculated from the integral of the peaks, which is shown in Table I. In PC-B3.2 and PC-B5.5, since the peaks are broad and overlap, integral values cannot be calculated accurately. The spectra in Fig. 5b cannot be used for integration because the area under the spectra does not correspond to the number of atoms due to NOE by proton irradiation.

It was shown from the far infrared and UV spectra that PC-B3.2 and PC-B5.5 have a polysilane skeleton consisting of Si–Si bonds. Silicon atoms forming the polysilane skeleton are determined quantitatively from the ^{29}Si NMR spectrum, that is, the characteristic peak at -34.48 ppm in PC-B3.2 and in PC-B5.5 in Fig. 5 should be due to ^{29}Si forming the polysilane skeleton, because the peak is between -20.50 ppm (HMDS) and -42.24 ppm (DMCHS). As shown in Table III, chemical analysis of the PCs shows that the quantities of oxygen in PC–TMS, PC-B3.2 and PC-B5.5 are far larger than in PC-470. Consequently, in the ^{29}Si NMR spectrum of each PC the silicon atom in the Si–O–Si bond should be considered. It is evident from Fig. 5 that the peak due to ^{29}Si with a siloxane bond should be between 6.45 ppm

TABLE II ^{29}Si NMR data of polycarbosilanes

	$\delta(^{29}SiC_4)$ (ppm)	$\delta(^{29}SiC_3H)$ (ppm)	$J_{^{29}Si-H}$ (Hz)	$\delta(^{29}SiC_xSi_{4-x})$ (ppm)
PC–TMS	−0.75	−17.50	182	–
PC-470	−0.75	−17.50	182	–
PC-B3.2	0.50	−16.01	180	−34.48
PC-B5.5	0.50	−16.43	180	−34.48

TABLE III Chemical compositions (wt%), empirical formulae and $\bar{M}_n$ of polycarbosilanes

	Si	C	H	O	B	Empirical formula	$\bar{M}_n$
PC–TMS	44.80	39.90	6.79	6.85		$SiC_{2.08}H_{4.24}O_{0.268}$	774
PC-470	48.18	39.92	6.85	0.81		$SiC_{1.77}H_{3.70}O_{0.038}$	1740
PC-B3.2	44.50	35.80	8.00	4.83	–	$SiC_{1.88}H_{5.03}O_{0.190}$	1738
PC-B5.5	44.90	39.20	7.44	6.20	0.093	$SiC_{2.04}H_{4.64}O_{0.242}B_{0.005}$	1312

(HMDSO) and −22.38 ppm (PDMSO); the peak at −34.48 ppm in PC-B3.2 and in PC-B5.5 is not in this range. The spectrum of PC–TMS has no peak around −34.48 ppm, so that the peak at −34.48 ppm is due to the silicon atom forming a polysilane skeleton in the molecule. The silicon atom does not couple with ^1H because the shape of the peak is not changed by proton irradiation. Consequently, this silicon atom should be bonded with at least one silicon atom and the rest of the bond should be with carbon atoms; it is called hereafter SiC_xSi_{4-x} ($x = 1$, 2 or 3). The peaks due to a silicon atom in a siloxane bond were not distinct, and could not be determined quantitatively. The ratio of SiC_xSi_{4-x} to ($SiC_4 + SiC_3H$) was calculated from the integral in the spectrum in Fig. 5a, which is given in Table I. The ratio of SiC_xSi_{4-x} in PC-B5.5 is smaller than in PC-B3.2, in accordance with the fact that the extinction coefficient K of PC-B5.5 is smaller than that of PC-B3.2.

From the results in Table I, the fractions of SiC_4, SiC_3H and SiC_xSi_{4-x} in each PC were calculated as follows. The fractions of SiC_4 and SiC_3H in PC–TMS and PC-470 can be calculated easily, using $SiC_xSi_{4-x} = 0$, as in Table IV. To calculate the fractions in PC-B3.2 and PC-B5.5, the following approximation was made. That is, the molecular structure of the PCs linear chain, and SiC_4, SiC_3H and SiC_xSi_4 are repetitions of the following structural units respectively:

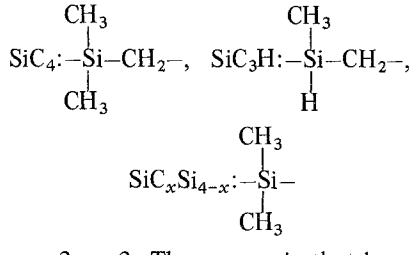

Here, $x = 2$ or 3. The reason is that because the polysilane skeleton is

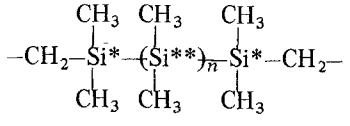

Si* and Si** correspond to SiC_3Si and SiC_2Si_2 respectively. In PC–TMS and PC-470, it will be confirmed whether the above approximation is valid. As shown in Table IV, the ratio of SiC_4:SiC_3H is 6.33:1 in PC–TMS and 1.04:1 in PC-470. By the above approximation, C–H/Si–H in PC–TMS and in PC-470 are 55.6 and 13.3 respectively; these values correspond to those in Table I. The approximation of the linear chain structure of PCs is thus shown to be effective. Using the value of C–H/Si–H in PC-B3.2 and in PC-B5.5, the fractions of SiC_4, SiC_3H and SiC_xSi_{4-x} are calculated as follows. First, from Table I, in PC-B3.2

$$(SiC_4 + SiC_3H):SiC_xSi_{4-x} = 1:0.159$$

Using the approximation,

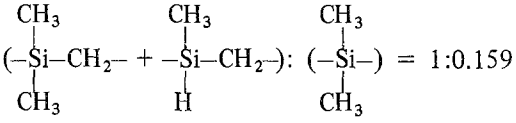

Consequently, because C–H/Si–H = 20.4,

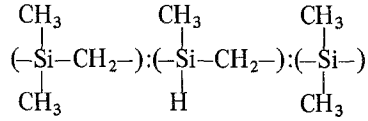

$$= 0.617:0.383:0.159$$

Similarly, in PC-B5.5

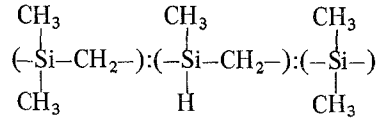

$$= 0.547:0.453:0.130$$

TABLE IV Fractions (%) of SiC_4, SiC_3H and SiC_xSi_{4-x} in polycarbosilanes

	SiC_4	SiC_3H	SiC_xSi_{4-x}
PC–TMS	86.4	13.6	0
PC-470	51.0	49.0	0
PC-B3.2	53.3	33.3	13.7
PC-B5.5	48.4	40.1	11.5

From the above results, in PC-B3.2

$$SiC_4:SiC_3H:SiC_xSi_{4-x} = 0.617:0.383:0.159$$

and in PC-B5.5

$$SiC_4:SiC_3H:SiC_xSi_{4-x} = 0.547:0.453:0.130$$

As shown in Table IV, each PC can be characterized through the three simple structural elements. On the basis of this result, the pyrolysis process and structure of the pyrolysis product will be discussed.

3.2. Characterization of the pyrolysis process of polycarbosilanes

The TG–DTA curve of each PC in nitrogen flow is shown in Fig. 6. It was reported previously that pyrolysis process can be discussed in three stages in the TG–DTA curves of PC–TMS and PC-470 [2]. In the present work, TG–DTA curves of PC-B3.2 and PC-B5.5 were measured, and further, as shown in Fig. 7, the gas evolution during pyrolysis of PCs in a vacuum was also measured. It was found that the pyrolysis process of PCs can be discussed with the divisions at temperature T_1, T_2, T_3, T_{4-1} and T_{4-2}, as in Table V. There are thus six stages in the pyrolysis process: up to T_1, T_1 to T_2, T_2 to T_3, T_3 to T_{4-1}, T_{4-1} to T_{4-2} and above T_{4-2}. The respective temperatures from T_1 to T_{4-2} were determined by the points of deflection in the TG curves in Fig. 6. The temperatures other than T_1 and T_2 were not distinct. Therefore, T_3 was determined as the termination temperature of an endothermic peak centred at temperature T_c in the DTA curve in Fig. 6. T_4 was divided into two, T_{4-1} as the initiation and T_{4-2} as the termination of a third peak of gas evolution observed in the temperature range of 1000 to 1200° C in Fig. 7. This temperature range corresponds to temperature ranges of the exothermic peaks observed in DTA curves of PC–TMS, PC-470 and PC-B5.5 in Fig. 6. Conversion mechanism into the inorganic by pyrolysis and structure of the product in each stage is discussed.

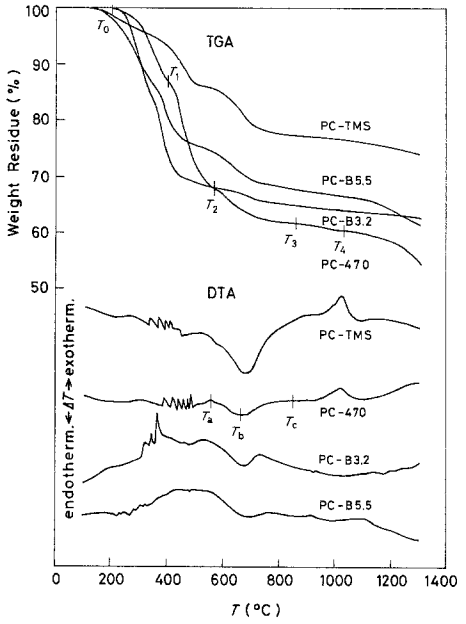

Figure 6 TG–DTA curves of polycarbosilanes in nitrogen flow.

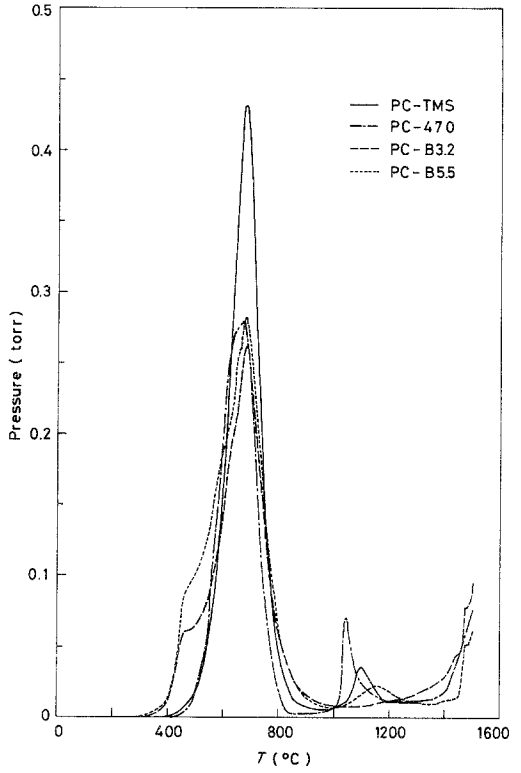

Figure 7 Gas evolution curves of polycarbosilanes in pyrolysis process.

3.2.1. The first and the second stage up to 550° C

The first stage up to T_1 of the pyrolysis process will be discussed. In this temperature range, although weight loss is large, gas evolution is small. No remarkable change is observed in the IR or far infrared spectra. Fig. 8 shows the changes in molecular weight distribution of PC–TMS heat treated at 350° C and of PC-470, PC-B3.2 and PC-B5.5 at 400° C. It is seen that the heat treatment above T_1 increases the high molecular weight components or shifts the molecular weight distribution

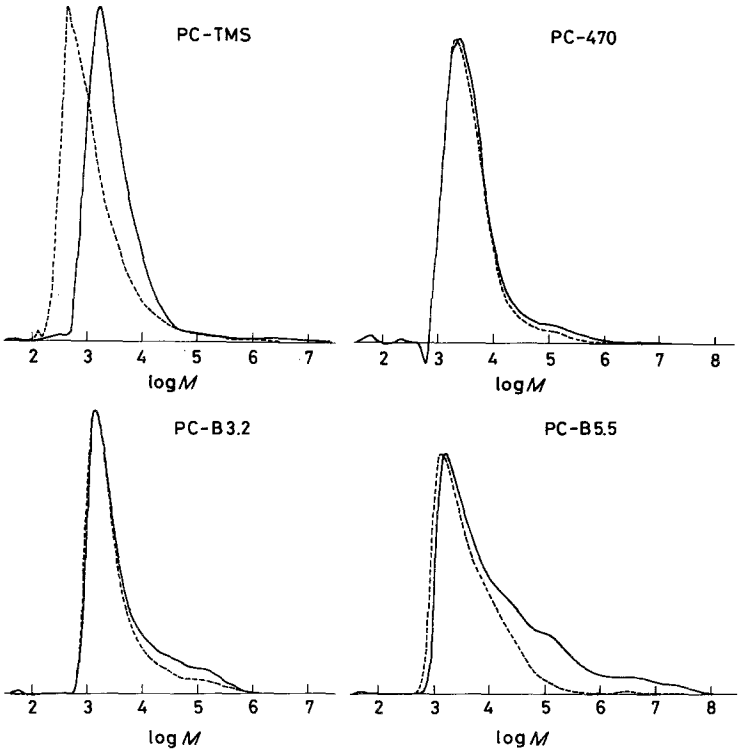

Figure 8 Molecular weight ($\bar{M}$) distributions of polycarbosilanes before (-----) and after (——) heat treatment.

to higher molecular weights. Since PC-470 was heat treated below T_1 (Table V), the molecular weight distribution is little changed.

The change due to the heat treatment below T_1 is mainly weight loss by evaporation of the low molecular weight polycarbosilane. Structural change of the PCs should start in the second stage.

In the second stage, T_1 to T_2, the molecular weight increases, as shown in Fig. 8. The weight loss in this stage is large as in the first stage in the TG curves of Fig. 6 and the gas evolution by pyrolysis is small, so that evaporation of the low molecular weight components is large. In this stage, however, PC-B3.2 and PC-B5.5 have a first gas evolution peak in Fig. 7, which is not observed in PC–TMS and PC-470. The mechanism in increase of the molecular weight of PC-3.2 and PC-B5.5 is thus different from that of PC–TMS and PC-470.

The relationship between $A\bar{\nu}/A_{2950}$ and heat-treatment temperature in each PC is shown in Fig. 9. In PC–TMS and PC-470, with increasing temperature, A_{2100}/A_{2950} decreases, A_{1250}/A_{2950} increases slightly and A_{1355}/A_{2950} is almost constant. It is indicated that, compared with the number of C–H bonds, the number of Si–H bonds decreases, that of Si–CH_3 bonds increases slightly and that of Si–CH_2–Si bonds is almost constant. Consequently, in this stage, the cross-linking with the Si–Si bond produced by dehydrogenation condensation between Si–H bonds is possible, for the gas evolution is observed above 300 to 400° C in Fig. 7. Particularly in PC–TMS, A_{2100}/A_{2950} at 500° C is half that at 300° C, which corresponds to the drastic increase in molecular weight of PC–TMS. Fritz *et al.* [6] explained the increase in molecular weight on the basis of the condensation accompanied by separation of low molecular weight hydrocarbon. Thus, the mechanism of increasing molecular weight in PC–TMS and PC-470 is the condensation between the molecules; the condensation in PC–TMS is rapid compared with that in PC-470.

In PC-B3.2 and PC-B5.5 in Fig. 9, with increasing temperature, A_{1250}/A_{2950}, A_{2100}/A_{2950} and A_{1355}/A_{2950} increase rapidly, so that the number of Si–CH_3, Si–H and Si–CH_2–Si bonds increases, compared with that of C–H bonds. However, it is impossible that the number of Si–CH_3 bonds becomes about twice that of C–H bonds when the

TABLE V Temperatures (°C) dividing the conversion process of polycarbosilanes into the inorganic by pyrolysis

	T_1	T_2	T_3	T_{4-1}	T_{4-2}
PC–TMS	330	540	860	960	1190
PC-470	400	565	860	920	1200
PC-B3.2	335	540	770	1100	1270
PC-B5.5	335	520	770	990	1350

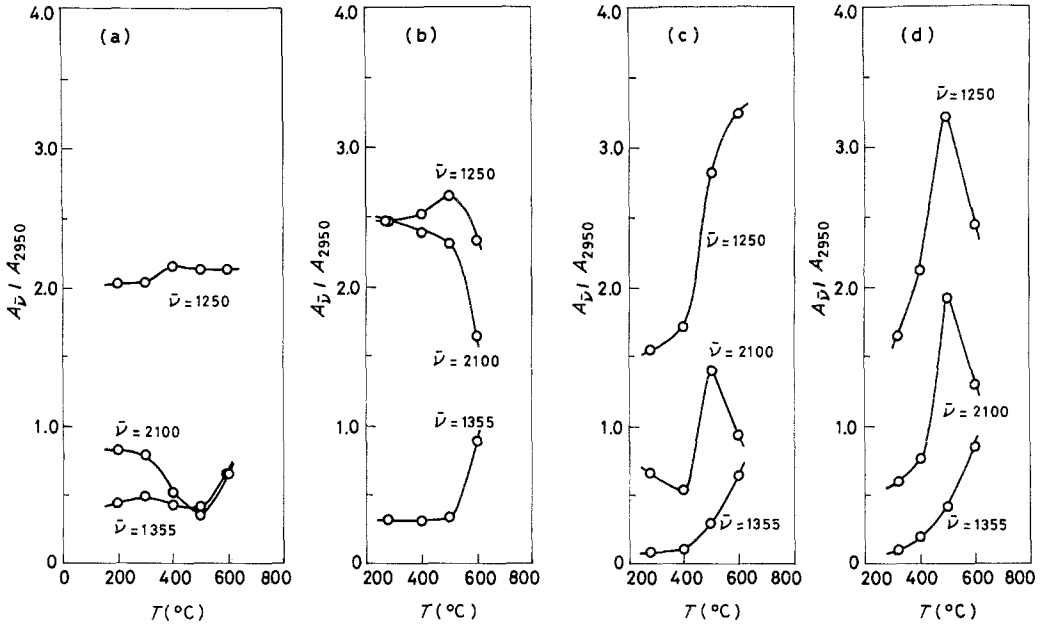

Figure 9 Changes in $A\tilde{\nu}/A_{2950}$ of polycarbosilanes in heat treatment: (a) PC–TMS, (b) PC-470, (c) PC-B3.2, (d) PC-B5.5.

number of Si–CH_2–Si bonds increases, because it is possibly only when Si–CH_2– Si bonds change into Si–$\overset{|}{C}$H–Si or Si–$\overset{|}{C}$–Si bonds. The absorbance (A) of absorption peaks, such as that for Si–CH_3 deformation, is a characteristic of the kind and structure of the compound even if the concentrations are the same. Therefore, the ratio of absorbances differs from one kind of compound to another. The values of A_{1250}/A_{2950} of polysilanes are generally low, 1.31 for PDMS and 1.22 for DMCHS. Then, as in Table IV, the reason the number of Si–CH_3 bonds becomes about twice that of C–H bonds by heat treatment is the existence of a polysilane skeleton in the molecule of PC-B3.2 and of PC-B5.5. The mechanism in increasing molecular weight of PC-B3.2 and of PC-B5.5 should be accompanied by a large change in the molecular structure. It was shown by the far infrared spectra that the peak due to the Si–Si bond in PC-B3.2 and in PC-B5.5 in Fig. 2 is almost annihilated by the heat treatment at 600° C. That is to say, the polysilane skeleton is decomposed up to about 600° C and converted into a carbosilane skeleton. Such a mechanism corresponds to the increase in Si–H and Si–CH_2–Si bonds with an increase in heat-treatment temperature, and can explain the rapid increase in A_{1250}/A_{2950}. A polysilane skeleton generally converts into a carbosilane skeleton in thermal decomposition and rearrangement. Hexamethyldisilane $Me_3SiSiMe_3$, for example, decomposes at 600° C [13], which is the highest temperature among polysilanes. Because of the radical reaction, radicals H· and Me· are produced in radical transfer, and so there arise hydrogen and methane gases, as observed in the first peak in the gas evolution curve. Therefore, the mechanism of increasing molecular weight is a combination of the high molecular weight radicals produced during the cleavage of the polysilane skeleton. From Fig. 8 it is evident that the increase in molecular weight is rapid in PC-B5.5 compared with that of PC-B3.2.

In the temperature range of T_1 to T_2 the molecular weight of the polycarbosilanes is increased. In PC–TMS and PC-470 the mechanism is the dehydrogenation and dehydrocarbonation condensation, and in PC-B3.2 and PC-B5.5 it is this condensation and the radical combination accompanied by change in the molecular structure. The increase in molecular weight is rapid in PC–TMS and PC-B5.5 as compared with those in PC-470 and PC-B3.2.

3.2.2. The third stage from 550 to 800° C

In the third stage T_2 to T_3, it is indicated from the TG–DTA and gas evolution curves that the hydrogens and the methyl groups in side chains of PCs are thermally decomposed. The largest gas evolution and a large endothermic peak are observed. This corresponds to the rapid decrease of the

absorption peaks of C–H (2950 cm^{-1}), Si–H (2100 cm^{-1}) and $Si–CH_3$ (1250 cm^{-1}) at 600° C and the annihilation of these peaks and the $Si–CH_2–Si$ (1355 cm^{-1}) peak at 800° C. It is evident in Fig. 9 that the $Si–CH_2–Si$ bond increases relatively, though the ratios of the absorbances at 600° C should have errors because the absorption peaks are broad and weak in Fig. 9. That is, the $Si–CH_2–Si$ bond should be produced by the reaction of Si–H and $Si–CH_3$. The main reaction during pyrolysis of organic polymers at high temperature is generally radical reaction. The bond energy of Si–H is the lowest in the polycarbosilane skeleton [6], so that the hydrogen radical is readily produced. Under the condition of the free radical reaction, the Si–C bond is relatively stable for homolytic fission and the C–H bond in $Si–CH_3$ is broken readily [14]. Thus, the primary steps in the decomposition are assumed to be:

$$-\overset{|}{\underset{|}{Si}}–H \xrightarrow{\Delta} -\overset{|}{\underset{|}{Si}}\cdot + \cdot H \quad (1)$$

$$-\overset{|}{\underset{|}{Si}}–CH_3 + \cdot H \rightarrow -\overset{|}{\underset{|}{Si}}–CH_2\cdot + H_2 \quad (2)$$

The formation of methane to an extent similar to that for hydrogen is observed [15], which is assumed to be:

$$-\overset{|}{\underset{|}{Si}}–CH_3 \xrightarrow{\Delta} -\overset{|}{\underset{|}{Si}}\cdot + \cdot CH_3 \quad (3)$$

$$-\overset{|}{\underset{|}{Si}}–CH_3 + \cdot CH_3 \rightarrow -\overset{|}{\underset{|}{Si}}–CH_2\cdot + CH_4 \quad (4)$$

Recombination of the radicals produced in Equations 1 and 2 should then lead to the $Si–CH_2–Si$ bond, besides H_2 and CH_4:

$$-\overset{|}{\underset{|}{Si}}\cdot + \cdot CH_2–\overset{|}{\underset{|}{Si}}– \rightarrow -\overset{|}{\underset{|}{Si}}–CH_2–\overset{|}{\underset{|}{Si}}– \quad (5)$$

$$-\overset{|}{\underset{|}{Si}}–CH_2\cdot + \cdot CH_2–\overset{|}{\underset{|}{Si}}– \rightarrow -\overset{|}{\underset{|}{Si}}–CH_2–CH_2–\overset{|}{\underset{|}{Si}}– \quad (6)$$

In Equation 6, it is to be noted that the $Si–CH_2–CH_2–Si$ bond may be produced. With increase of the heat-treatment temperature, formation of the network and three-dimensional structure should occur by the reaction with $–CH_2–$ in the $Si–CH_2–Si$ bond:

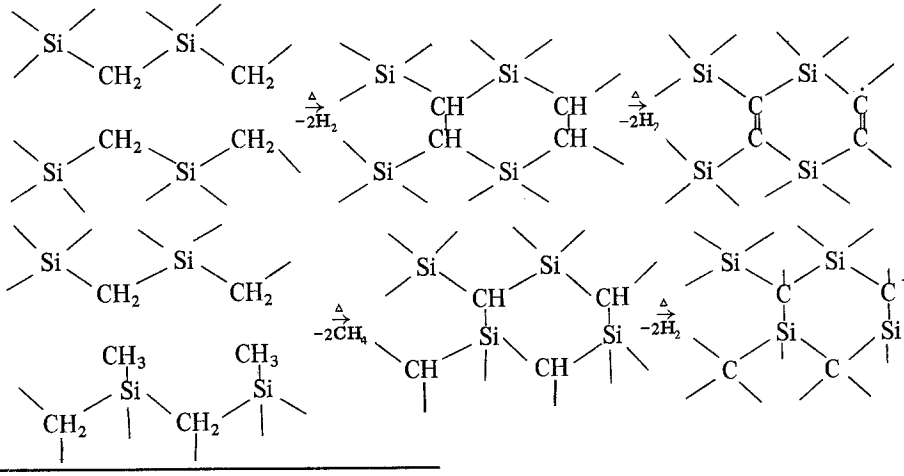

(7)

(8)

Reaction 7 explains the phenomenon that each PC becomes light brown at 600° C and then blackish with increase of the heat-treatment temperature up to about 800° C. And this corresponds to the expansion of the conjugated system in the production of C=C.

In the third stage, PCs are converted into inorganic structure with network and three-dimensional structure by the decomposition of Si–H and C–H in $SiCH_3$ and $Si–CH_2–Si$ bonds, such as dehydrogenation and demethanation. In this stage, it is to be noted that the C–C bond is formed in the inorganic structure.

3.2.3. The fourth and the fifth stage from 800 to 1200° C

In the fourth stage from T_3 to T_{4-1}, the gas evolution by thermal decomposition is almost complete; the stage precedes the next stage of gas evolution. It is observed in IR spectra, however, that the characteristic structural change is little. Each PC heat treated at 800° C only shows peaks in the bands of 820 cm^{-1} (Si–C stretch), 1020 cm^{-1} (CH_2 wagging in $Si–CH_2–Si$) and 460 cm^{-1} (Si–O–Si deformation) and the peak in the band of

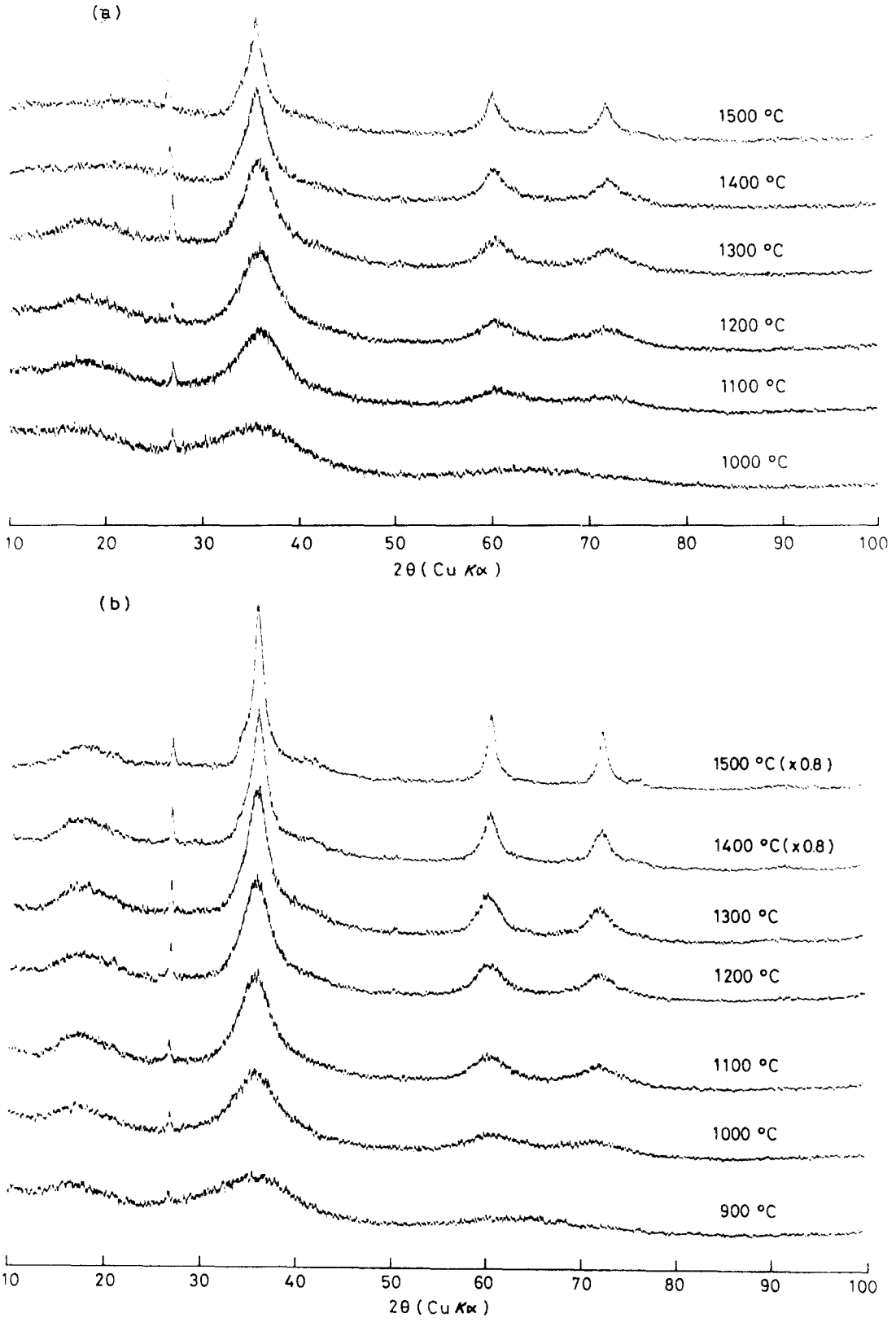

Figure 10 X-ray diffraction patterns of polycarbosilanes heat treated in a vacuum: (a) PC–TMS, (b) PC-470, (c) PC-B3.2, (d) PC-B5.5.

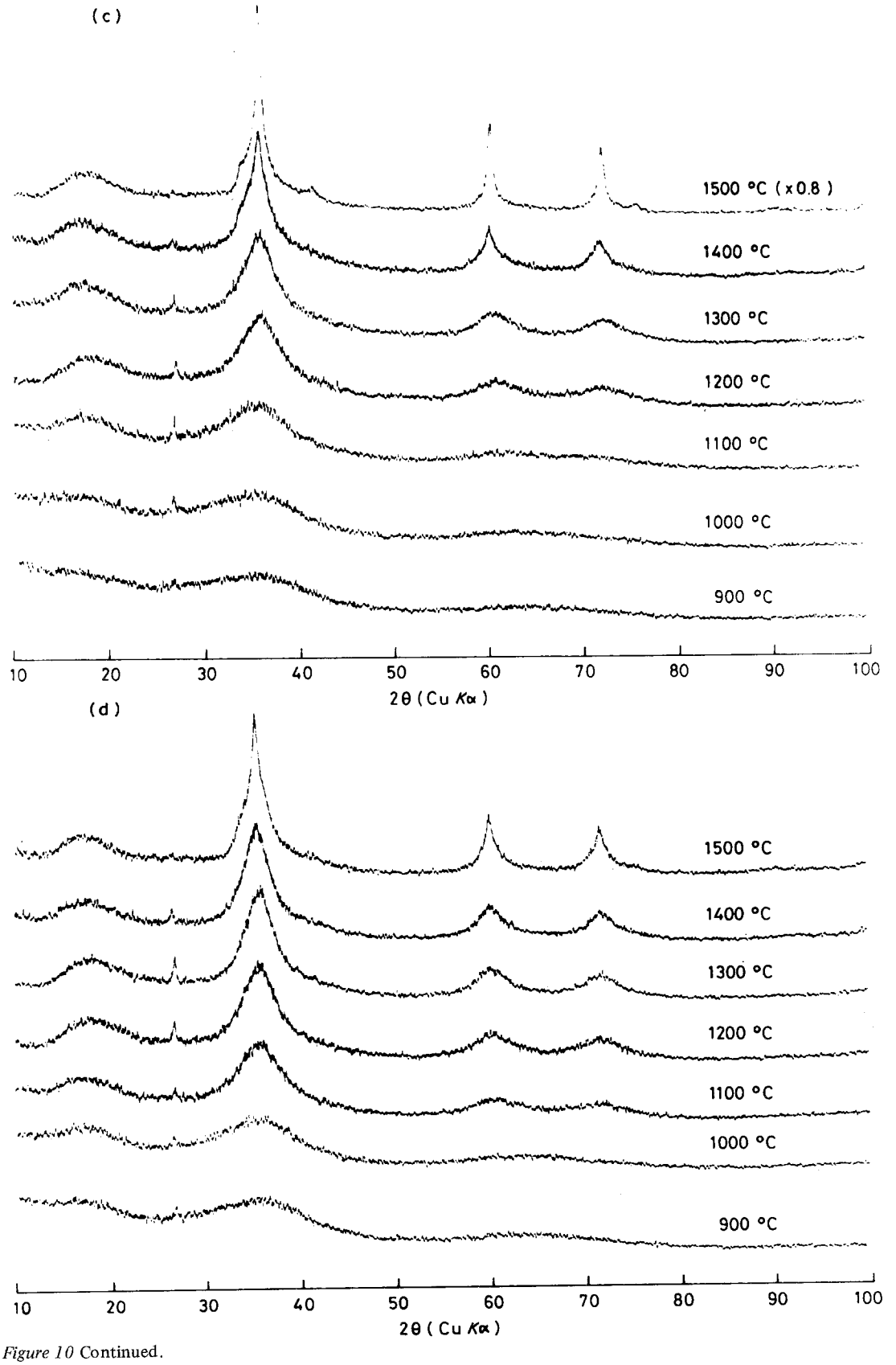

Figure 10 Continued.

1020 cm^{-1} shifts to 1080 cm^{-1} (Si–O stretch) [16] with increase of the temperature. As shown in Fig. 10, the X-ray powder diffraction patterns of PCs heat treated at 900° C or above, below T_{4-1} show no separation of the diffraction peaks (220) and (311) of β–SiC, so that the products should be in amorphous structure. This stage is assumed to be transitional toward the fifth stage.

In the fifth stage from T_{4-1} to T_{4-2}, the third peak in the gas evolution curve is characteristic. This gaseous product is hydrogen [15]. In the X-ray powder diffraction patterns of Fig. 10, above T_{4-1} the diffraction peaks (220) and (311) of β–SiC are separate and are narrower. In this stage, an exothermic peak is observed in the DTA curves of PC–TMS, PC-470 and PC-B5.5 in Fig. 6, indicating crystallization of β–SiC. In IR spectra the peak due to Si–C stretching shifts to higher wave numbers with increase of the heat-treatment temperature, which shows that the Si–C bond becomes tight. Gas evolution thus occurs and the amorphous structure of the pyrolysis product becomes a crystalline structure. In Table VI, chemical analysis of the pyrolysis products at 1300° C shows that the crystalline products are nonstoichiometric with excess carbon in all polycarbosilanes. The structure of the carbon is not known. Since the crystallization occurs with dehydrogenation in this temperature range, production of the excess carbon and crystallization may be due to Equations 7 and 8.

The absorption peaks at 1080 and 460 cm^{-1} in IR spectra and chemical analysis show that SiO_2 exists in the products. As shown in the IR spectra of Fig. 11, SiO_2 in the product of PC-470 by heat treatment at 1300° C is largely removed by HF treatment. By this treatment, as shown in Fig. 12, the diffraction peak of $2\theta = 26.63°$ in the powder X-ray diffraction pattern is annihilated, but not by heat treatment in air at 600 to 700° C, so that the peak is not a (002) diffraction line of carbon. Consequently, the peak at $2\theta = 26.63°$ is due to a (101) diffraction line [17] of the α-quartz; it is observed from the fourth stage in all PCs.

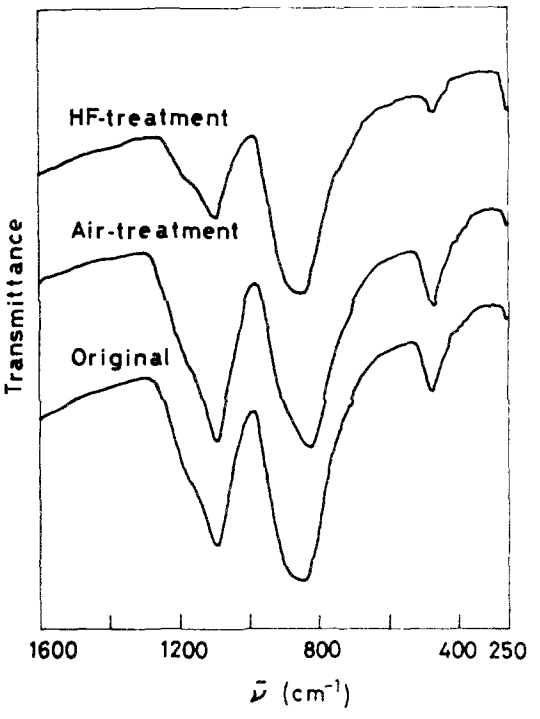

Figure 11 IR spectra of PC-470 heat treated at 1300° C before and after air treatment and after HF treatment.

In this stage, each PC is converted completely from the organic into the inorganic by dehydrogenation and β–SiC is crystallized. Composition of the products is nonstoichiometric with excess carbon and a little α-quartz.

3.2.4. The sixth stage above 1200° C

In the sixth stage above T_{4-2}, there again appears a gas evolution peak, as shown in Fig. 7. The gas is CO [15]. In this stage, the powder X-ray diffraction patterns in Fig. 10 become sharp with increase of the heat-treatment temperature, so that crystal growth must occur. Further, in PC-B3.2 and PC-B5.5, the (101) diffraction line of α-quartz at $2\theta = 26.5°$ is annihilated, corresponding to the rapid decrease of Si–O bond (1080 cm^{-1}) in the IR spectra of PC-B3.2 and PC-B5.5 by heat treatment above 1300° C. That is, in this stage, the Si–O bond in the product reacts with the excess

TABLE VI Chemical compositions (wt%) and empirical formulae of pyrolysis products of polycarbosilanes at 1300° C in a vacuum

	Si	C	H	O	B	Empirical formula
PC–TMS	52.4	40.1	0.07	5.73		$SiC_{1.79}H_{0.037}O_{0.191}$
PC-470	60.3	36.1	0.10	1.31		$SiC_{1.40}H_{0.046}O_{0.038}$
PC-B3.2	56.3	35.7	0.28	4.67	0.005	$SiC_{1.48}H_{0.139}O_{0.145}$
PC-B5.5	54.5	36.6	0.10	4.53	0.12	$SiC_{1.57}H_{0.051}O_{0.145}B_{0.006}$

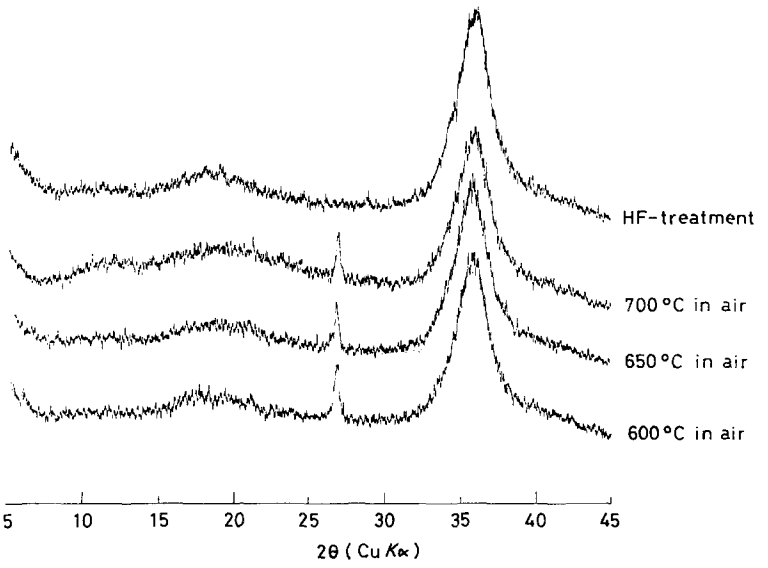

Figure 12 X-ray diffraction patterns of PC-470 heat treated at 1300° C after air treatment and after HF treatment.

carbon and the Si–C bond is formed with CO gas evolution. In PC–TMS and PC-470, however, the (101) diffraction line remains even at the heat-treatment temperature of 1500° C; in IR spectra, the decrease of Si–O bond is not rapid even at 1500° C, compared with the case of PC-B3.2 and PC-B5.5. As seen, the reaction of Si–O bond with excess carbon is more rapid in PC-B3.2 and PC-B5.5 than in PC–TMS and PC-470, possibly because the state of existence of the Si–O bond and of the excess carbon are different between these two groups.

The relationship between L_{111} and heat-treatment temperature is shown in Fig. 13. At 1500° C L_{111} of the pyrolysis product increases in the order of PC–TMS < PC-B5.5 < PC-470 < PC-B3.2. Crystal growth is observed in the fifth stage and further in the sixth stage; the growth in the fifth stage L_{111} is only slight and in the sixth stage L_{111} it is rapid. The apparent crystalline size of β–SiC in the pyrolysis product at 1500° C is considerably different among PCs. This is similar to pyrolysis of the organic compounds; phenolic resins and cellulose carbonized in solid phase are non-graphitizable carbons, and pitches carbonized in liquid phase are graphitizable carbons. Though the reaction above about 500° C is in solid phase in both cases, it influences significantly the carbonization process whether in early carbonization below 500° C molecules of the organic compound are mobile and are easily stacked in liquid phase or molecules are not mobile and are hardly stacked. In Fig. 8, which shows the change of the molecular weight distribution during heat treatment, PC–TMS is rapidly condensed between the molecules at 350° C and in PC-B5.5 the increase in higher molecular weight is remarkable at 400° C. On the other hand, though the difference is not distinct between PC-470 and PC-B3.2, at 400° C the peak of the molecular weight distribution is in lower molecular weight and more sharp in PC-B3.2 than in PC-470. Consequently, in the pyrolysis process, the molten PC-B3.2 should have lower viscosity than that of molten PC-470 and have a higher transition temperature into the solid phase than that of PC-470. Each PC melts by heating and is converted into the inorganic through the liquid phase in early stage of the pyrolysis process. The transition temperature from liquid pahse to solid phase should increase in the order of PC–TMS <

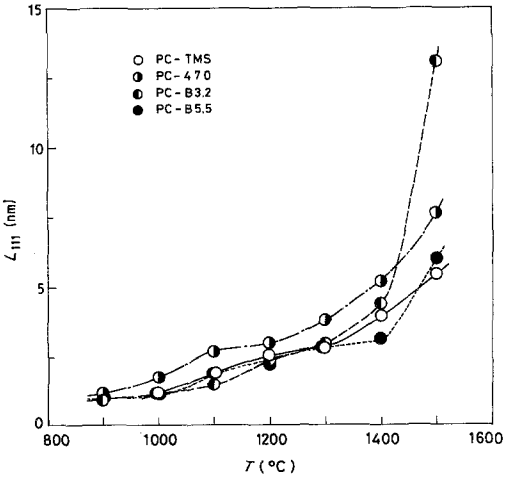

Figure 13 Apparent crystalline sizes of β–SiC (L_{111}) in polycarbosilanes heat treated in a vacuum.

PC-B5.5 < PC-470 < PC-B3.2. At 1500° C, the crystal growth of β–SiC is depressed in PC–TMS and accelerated in PC-B3.2.

In the sixth stage, crystal growth of crystalline β–SiC formed in the fifth stage occurs and Si–O bonds in the product decrease. The reaction between Si–O bonds and excess carbon is more rapid in PC-B3.2 and PC-B5.5 than in PC–TMS and PC-470. In the pyrolysis process of PCs, the transition temperature from liquid phase to solid phase in increase of the molecular weight by heating increases in the order of PC–TMS < PC-B5.5 < PC-470 < PC-B3.2. Consequently, the crystalline size of β–SiC at 1500° C increases in this order, because when the liquid phase is maintained at higher temperature the molecules are mobile and tend to condense into the skeleton to form a β–SiC structure.

4. Conclusion

In each PC, from the measurements of the substituents on a silicon atom, and the silicon atoms forming the PC skeleton were represented by means of three simple elements; silicon bonded with four carbon atoms (SiC_4), silicon bonded with one hydrogen atom and three carbon atoms (SiC_3H), and silicon bonded with x carbon atoms and $(4-x)$ silicon atoms (SiC_xSi_{4-x}, $x = 1$, 2 or 3). The differences in fractions of these silicon atoms among PCs are important in discussion of the conversion process of PCs into the inorganic and of the differences in structure of the pyrolysis products.

The conversion process of PCs into silicon carbide can be divided in six temperature ranges. Structures of the pyrolysis products in each stage were studied comparatively. Following are the results, which are summarized in Fig. 14.

In the first stage, in each PC, weight loss occurs due to evaporation of the low molecular weight components and the number average molecular weight increases without structural change.

In the second stage, the molecular weight increases in each PC. The mechanism is dehydrogenation and dehydrocarbonation condensation in PC–TMS and PC-470 and this condensation and the radical polymerization due to pyrolysis of the polysilane skeleton of molecule in PC-B3.2 and PC-B5.5.

In the third stage, by decomposition of the side chains of PC, such as dehydrogenation and demethanation, PC is converted into the inorganic structure with a network and three-dimensional structure. In the skeleton of inorganic structure are Si–C and C–C bonds.

The fourth stage is transitional toward the fifth stage. The products are amorphous structure.

In the fifth stage, β–SiC is crystallized with dehydrogenation. Compositions of the products are nonstoichiometric with excess carbon, containing a little α-quartz. The apparent crystalline sizes of β–SiC are 2 to 3 nm.

In the sixth stage, crystal growth of crystalline β–SiC formed in the fifth stage occurs. Si–O bonds in the products decrease by the reaction between Si–O bonds and excess carbon. The reaction is more rapid in PC-B3.2 and PC-B5.5 than in PC–TMS and PC-470. Crystal growth increases in the order of PC–TMS < PC-B5.5 < PC-470 < PC-B3.2, because the transition temperature from liquid pahse to solid phase in the pyrolysis process increases in this order.

In the next report, the conversion process of the cured PC fibre into SiC fibre by pyrolysis will be described in detail.

References

1. S. YAJIMA, Y. HASEGAWA, J. HAYASHI and M.

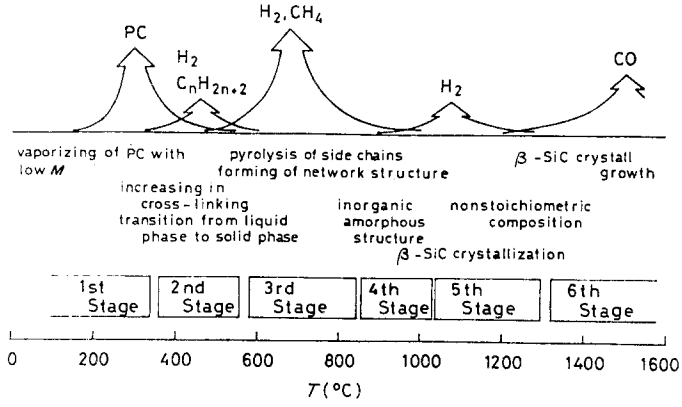

Figure 14 Conversion process of polycarbosilanes into the inorganic by pyrolysis.

IIMURA, *J. Mater. Sci.* **13** (1978) 2569.
2. Y. HASEGAWA, M. IIMURA and S. YAJIMA, *ibid.* **15** (1980) 720.
3. S. YAJIMA, Y. HASEGAWA, K. OKAMURA and T. MATSUZAWA, *Nature* **273** (1978) 525.
4. S. YAJIMA, K. OKAMURA, J. TANAKA and T. HAYASE, *J. Mater. Sci.* **16** (1981) 3033.
5. S. YAJIMA, K. OKAMURA, T. MATSUZAWA, Y. HASEGAWA and T. SHISHIDO, *Nature* **279** (1979) 706.
6. G. FRITZ, J. GROBE and D. KUMMER, *Adv. Inorg. Chem. Radiochem.* **7** (1965) 349.
7. C. G. PITT, M. M. BURSEY and P. F. ROGERSON, *J. Amer. Chem. Soc.* **92** (1970) 519.
8. R. WEST and A. INDRIKSONS, *ibid.* **94** (1972) 6110.
9. R. WEST and E. CARBERRY, *Science* **189** (1975) 179.
10. G. FRITZ, W. KEMMERLING, G. SONNTAG, H. J. BECHER, E. A. V. EBSWARTH and J. GROBE, *Z. Anorg. Allg. Chem.* **321** (1963) 10.
11. D. R. WEYENBERG and L. E. NELSON, *J. Org. Chem.* **30** (1965) 2618.
12. G. FRITZ and E. MATERN, *Z. Anorg. Allg. Chem.* **426** (1976) 28.
13. K. SHIINA and M. KUMADA, *J. Org. Chem.* **23** (1958) 139.
14. C. EABORN and B. W. BOTT, "Organometallic Compounds of the Group IV Elements" Vol. 1, edited by A. G. MacDiarmid (Dekker, 1968) Pf. 2, pp. 350–9.
15. T. MATSUZAWA, private communication.
16. M. DECOTTIGNIES, J. PHALIPPOU and J. ZARZYCKI, *J. Mater. Sci.* **13** (1978) 2605.
17. Powder Diffraction File, Card No. 5-490, Joint committee for Powder Diffraction Standards, Swarthmore, Pennsylvania (1960).

Received 7 March
and accepted 24 March 1983